

# Fatigue and Fracture Behavior of affordable Ti-B Alloys

**Final Report Submitted to the  
Asian Office of the Aerospace Research & Development**

by

Dr. U. Ramamurty  
Assistant Professor  
Department of Metallurgy  
Indian Institute of Science  
Bangalore – 560 012, INDIA

**in collaboration with**

Indrani Sen, PhD Student, IISc  
and  
D. Miracle and S. Tamirisa  
AFRL, Wright Patterson Air Force Base, Dayton, OH, USA

**April 2006**

# Report Documentation Page

*Form Approved  
OMB No. 0704-0188*

Public reporting burden for the collection of information is estimated to average 1 hour per response, including the time for reviewing instructions, searching existing data sources, gathering and maintaining the data needed, and completing and reviewing the collection of information. Send comments regarding this burden estimate or any other aspect of this collection of information, including suggestions for reducing this burden, to Washington Headquarters Services, Directorate for Information Operations and Reports, 1215 Jefferson Davis Highway, Suite 1204, Arlington VA 22202-4302. Respondents should be aware that notwithstanding any other provision of law, no person shall be subject to a penalty for failing to comply with a collection of information if it does not display a currently valid OMB control number.

1. REPORT DATE <b>02 AUG 2006</b>	2. REPORT TYPE <b>Final Report (Technical)</b>	3. DATES COVERED <b>23-05-2006 to 02-08-2006</b>			
4. TITLE AND SUBTITLE <b>Fatigue and fracture behavior of affordable Ti-B alloys</b>		5a. CONTRACT NUMBER <b>FA520905P0467</b>			
		5b. GRANT NUMBER			
		5c. PROGRAM ELEMENT NUMBER			
6. AUTHOR(S) <b>Upadrasta Ramamurty</b>		5d. PROJECT NUMBER			
		5e. TASK NUMBER			
		5f. WORK UNIT NUMBER			
7. PERFORMING ORGANIZATION NAME(S) AND ADDRESS(ES) <b>Indian Institute of Science, Department of Metallurgy, Bangalore 560 012, India, ZZ, 560012</b>		8. PERFORMING ORGANIZATION REPORT NUMBER			
9. SPONSORING/MONITORING AGENCY NAME(S) AND ADDRESS(ES) <b>The US Research Labolatory, AOARD/AFOSR, Unit 45002, APO, AP, 96337-5002</b>		10. SPONSOR/MONITOR'S ACRONYM(S) <b>AOARD/AFOSR</b>			
		11. SPONSOR/MONITOR'S REPORT NUMBER(S) <b>AOARD-054034</b>			
12. DISTRIBUTION/AVAILABILITY STATEMENT <b>Approved for public release; distribution unlimited</b>					
13. SUPPLEMENTARY NOTES					
14. ABSTRACT <b>In this project, we have examined the mechanical properties of the Ti-6Al-4V alloy with varying amounts of B content. The cast and HIPed alloys with 0.05, 0.10 and 0.4 wt.% B additions were supplied by Tamirisa and Miracle of AFRL, WPAFB. Microstructural observations indicate that the B addition reduces the as-cast grain size dramatically. Concomitantly, an increase in the yield and ultimate tensile strengths was observed. Fracture toughness measurements indicate a reduction in K<sub>Ic</sub> values with increasing B content, owing primarily to the reduced grain size. Fatigue crack growth measurements show a gradual reduction in threshold for fatigue crack initiation. Fractographic analyses were conducted to examine the micromechanical reasons for the observed trends.</b>					
15. SUBJECT TERMS <b>Titanium Alloy, Fatigue and Fracture</b>					
16. SECURITY CLASSIFICATION OF:			17. LIMITATION OF ABSTRACT	18. NUMBER OF PAGES <b>20</b>	19a. NAME OF RESPONSIBLE PERSON
a. REPORT <b>unclassified</b>	b. ABSTRACT <b>unclassified</b>	c. THIS PAGE <b>unclassified</b>			

## **Abstract**

In this project, we have examined the mechanical properties of the Ti-6Al-4V alloy with varying amounts of B content. The cast and HIPed alloys with 0.05, 0.10 and 0.4 wt.% B additions were supplied by Tamirisa and Miracle of AFRL, WPAFB. Microstructural observations indicate that the B addition reduces the as-cast grain size dramatically. Concomitantly, an increase in the yield and ultimate tensile strengths was observed. Fracture toughness measurements indicate a reduction in  $K_{Ic}$  values with increasing B content, owing primarily to the reduced grain size. Fatigue crack growth measurements show a gradual reduction in threshold for fatigue crack initiation. Fractographic analyses were conducted to examine the micromechanical reasons for the observed trends.

## **1. Introduction**

Titanium alloys, particularly Ti-6Al-4V (referred here afterwards as Ti64), are extensively used in the aerospace propulsion systems and there is a continuous drive to enhance their structural efficiency through enhanced alloy design that gives improved mechanical properties. The addition of a small amount of B (less than 2 wt.%) to Ti alloys was shown to improve the specific stiffness and strength significantly. However, a major drawback of these alloys is the ductility, which is only about 2%. It was recently discovered that the addition of ~0.4 wt.% B to the Ti64 reduces the as-cast grain size considerably. For example, the grain size in the as-cast Ti64-0.4B is ~100 microns whereas it is ~1700 microns in Ti64 that is processed in exactly the same manner. This reduced grain size has a strong economic advantage, as it obviates the need for several thermomechanical processing steps that are necessary to breakdown the as-cast coarse grain structure. Microstructural studies show that the TiB needles, about a micron in size, restrict the grain growth.

In addition to the promise of a marked reduction in the cost of processing Ti-alloy components, trace addition of B were also shown to improve the uniaxial tensile properties considerably. About 10% enhancement in elastic modulus, yield and ultimate tensile strengths, as compared to those alloys without B, were observed. However, detailed mechanical property characterization and understanding the connections between the microstructure and properties is yet to be carried out. In particular, the fatigue crack

growth and fracture properties, which are highly sensitive to the microstructure near the threshold regime, need to be evaluated, which is the objective of this project. These are important since the Ti alloy components are subject to fatigue loading conditions in service. Specific objectives of this project (as listed in the proposal) are as following:

- a) Study the variation of the fracture toughness with the grain size and understand the micromechanisms responsible for the observed variation, if any.
- b) Examine the effect of grain size on the room temperature fatigue crack growth behavior, with specific focus on the near-threshold fatigue crack growth regime, which is highly sensitive to the microstructure.

## **2. Materials and Experiments**

75 mm diameter ingots, cast and hot isostatically pressed (HIPed) with nominal compositions of Ti-6Al-4V-xB (with x values of 0.05, 0.1 and 0.4 wt.%) were supplied by Dr. Sesh Tamirisa of AFRL, WPAFB. For the tensile testing, 35 mm gage length dog-bone shaped specimens with 6 mm width and 2 mm thickness were electro-discharge machined (EDM) from the as-received billets. Tensile tests were conducted in an Instron machine with a strain rate of 0.001/s. Fracture toughness,  $K_{Ic}$  and fatigue crack growth experiments were carried out at a temperature of 21°C on chevron-notched half C(T) specimens of 24mm width and 12 mm thickness as per the ASTM standard E 399-90. The samples were pre-cracked with an applied load amplitude,  $\Delta P$ , of 4500 N. The load ratio,  $R$  (ratio of the minimum to maximum loads of the fatigue cycle), and the frequency,  $\nu$ , were maintained 0.1 and 10 Hz, respectively. For the  $K_{Ic}$  measurements, the pre-crack length was such that the  $a/W$  ( $a$  is the total crack length) ratio is  $\sim 0.5$ . Subsequently, samples were pulled until fracture at a rate of 0.1 mm/s. The fatigue crack growth experiments were conducted on the pre-cracked samples as per the ASTM standard E 647-05. Here also the  $R$  and  $\nu$  were kept at 0.1 and 10 Hz, respectively. Crack growth was monitored using a traveling microscope. For practical purposes, the threshold for the fatigue crack initiation,  $\Delta K_0$ , was defined as the  $\Delta K$  at which no crack growth was observed after 10,000 cycles.

Hardness was measured using an instrumented microhardness tester (CSM) with Vickers indenter at room temperature. For this, specimens of size 12mm\*12mm\*10mm

were cut, metallographically polished and etched with Kroll's reagent. The load used for the indentation is 5 N with a loading/unloading rate of 0.083 N/s with pause time at peak load of 10 s. 10 indentations for each sample were performed and the mean values are reported. Metallographic examinations of the alloys were conducted after polishing and etching with Kroll's reagent. Fractography was conducted using a scanning electron microscope (SEM).

### 3. Results and Discussion

#### 3.1. Microscopy

Figures 1 a-c show the optical micrographs of the 0.05, 0.1 and 0.4 wt.% B containing Ti64 alloy. Higher magnification Scanning electron micrographs (Fig. 2) show that needle shaped TiB particles with aspect ratio of 2.8 (approximately) are at the grain boundaries forming a necklace like arrangement. This network is more prominent for Ti64-0.4B. The presence of TiB needle is confirmed by EDAX. The grain size was plotted in Fig. 3 as a function of the B content. Here, the base Ti64 without any B data was obtained from literature [4]. It is seen that the addition of B reduces the grain size,  $d$ , quite dramatically, by an order of magnitude, even with a relatively small addition of 0.05 wt.% B. Although higher amounts of B additions further reduce the grain size, the reduction is only marginal. Fig. 3 also shows that the  $\alpha$  lath size,  $\lambda$ , also decreases, concomitant with the grain size, due to the addition B.  $\alpha$  lath size value in Ti64 with no B in it, is considered from literature [2]. The average values of  $d$  and  $\lambda$  are listed in the table.

#### 3.2. Tensile properties

Fig. 4 shows the tensile stress-strain graphs of Ti64 containing 0.05, 0.1 and 0.4 wt.% B. The variation of yield strength,  $\sigma_y$ , and ultimate tensile strength,  $\sigma_U$ , with the B addition is shown in Fig. 5. The literature [4] values of Ti64 without B are also plotted. It is seen that there is a continuous increase in both  $\sigma_y$  by about 16% and  $\sigma_U$  by about 13% from Ti64 with no B addition to Ti64-0.4B. This enhancement in tensile properties can solely be attributed to the reduction in grain size, as the Ti64 is essentially elastic-perfectly plastic (i.e. very low work hardening rate,  $n$ ). The latter can be seen from Fig. 6, wherein

$n$  is plotted a function of wt.% B. Although a continuous reduction is seen, the absolute values are very small, and hence it can be concluded that the strain hardening behavior of Ti64 essentially remains unchanged with the addition of B. The strain at failure,  $\epsilon_f$ , appears to decrease with the B addition. However, this reduction is as not precipitous as in the hypereutectic Ti64-B alloys wherein the ductility reduces below the critical minimum (for applications in aerospace structures) of 5%.

Concomitant with the increase in  $\sigma_U$ , the Vickers hardness,  $H_V$ , was also found to increase by about 26%, with increasing amount of B (Fig. 7) due to the presence of hard TiB phase at the grain boundaries. Here the hardness of Ti64 with no B addition is found from literature [1].

### 3.3. Fracture toughness

Fracture toughness is found to decrease with the increase in amount of B added. This variation is plotted in Fig. 8. It has been found that the fracture toughness values decreases by 75% from the value of  $152 \text{ MPa m}^{0.5}$  in Ti64 with no B addition [2], to  $38 \text{ MPa m}^{0.5}$  in Ti64-0.4B. Moreover, although a continuous decrease in the fracture toughness values are seen for increase in amount of B addition in Ti64, the maximum reduction of about 52% is observed for Ti64-0.05 B having the value of  $72.9 \text{ MPa m}^{0.5}$ . This vast reduction is mainly associated with the reduction in grain size from  $1700 \mu\text{m}$  to  $233.4 \mu\text{m}$  with only 0.05 wt% of B addition. This behavior of reduction in fracture toughness values with the reduction in grain size can be explained with the help of RKR (Ritchie, Knott and Rice) model. According to [6], failure at low temperature has been modeled as slip-initiated cleavage fracture. This cleavage cracks propagate in an unstable manner when the maximum principal tensile stress ( $\sigma_{\text{max}}$ ), ahead of the stress concentrator exceeds a critical value ( $\sigma_f$ ). The RKR model proposes that at low temperature when this local tensile stress ( $\sigma_{\text{max}}$ ) exceeds a critical fracture stress ( $\sigma_f$ ) over a microstructurally significant characteristic size-scale ( $l_0^*$ ), which lies between  $2d$  to  $4d$  ( $d$  is the grain size),  $\sigma_{\text{max}}$  leads to  $K_{IC}$ . Since  $K_{IC}$  is directly proportional to  $l_0$ , so the fracture toughness values get reduced, as the grain size is refined with the addition of B in Ti64. Thus a large reduction in grain size for only 0.05 wt% B addition leads to a

dramatic decrease in the fracture toughness and hence an overall decrease in fracture toughness is also associated with increasing B content.

Fractographs at high magnification of 2000x (Fig. 10 a-c) shows the presence of some dimples in the fracture surface of Ti64-0.05 TiB whereas water marks in Ti64-0.1B and Ti64-0.4B indicating that the alloy is getting more and more brittle with increasing wt % of B addition. This brittleness may be due to the presence of more and more hard and brittle TiB phase with increasing B addition in Ti64.

### 3.5. Fatigue crack growth

Fatigue crack growth of Ti64-0.1B and Ti64-0.4B are measured with an Instron machine following the stress intensity factor range ( $\Delta K$ ) shedding method, by 10% reduction in  $\Delta K$  value for every 0.5 mm of crack growth to reach the threshold stress intensity factor range,  $\Delta K_0$ , (corresponds to  $dn > 100000$  cycles for 0.1 mm of crack growth). After reaching the threshold, the tests were continued at constant load range. The values of  $\Delta K_0$  along with the Paris exponent,  $m$  are listed in the table. SEM of the crack propagation path, shown in Fig. 12, suggests that the crack has a to deviate along the  $\alpha$  laths at the near threshold region, and the widmanstatten structure leads to slow crack growth. Moreover as it has been found from literature [2,7], the crack growth rate actually decreases as the grain, colony and lath size increases due to increased crack branching, crack deflection along the laths and secondary cracks formation, all of which lead to fracture surface roughness. The crack growth rate vs. the stress intensity factor range for the composition, plotted in Fig. 11, also shows a slightly decreased fatigue crack growth rate for Ti64-0.1 B compared to Ti64-0.4B, but since the refinement is not too large with 0.4 wt% B addition in Ti64 compared to 0.1 wt% B addition in it, the reduction in the crack growth rate is small. It is also evident from the table that as the grain size is refined with increased B addition to Ti64, the threshold stress intensity factor range actually decreases. The fractured surface of the specimens also shows much roughness in Ti64-0.1B compared to Ti64-0.4B. This surface roughness is associated with more crack deflection in coarser grain sized specimen. It has also been found from literature [8] that as  $R$  increases in fatigue crack growth curves, the crack growth rate increases as well as the threshold  $\Delta K_0$  decreases but since we have done all the experiment at same  $R$  of 0.1,

the increment in the fatigue crack growth rate and the reduction in threshold stress intensity range is solely due to the grain refinement of Ti64 with increased addition of B in it.

#### 4. Conclusions

B addition in Ti64 reduces the as-cast grain size dramatically by about an order of magnitude, as a result of which an increase in the yield and ultimate tensile strengths and hardness were observed. There is a reduction in fracture toughness,  $K_{Ic}$  with increasing B content, also due to the reduced grain size. Fatigue crack growth measurements show a gradual reduction in threshold for fatigue crack initiation as well as slight increase in the fatigue crack growth rate with B addition in Ti64 again due to the grain refinement.

#### **Acknowledgements**

We acknowledge the assistance rendered by S. Sasidhara, N. Eswara Prasad, and K. Mahesh in various experiments reported in this work.

#### **References**

1. K. Euh et al., Scripta Materialia 45 (2001), 1
2. V. Sinha et.al., Materials Science and Engineering A, 319-321 (2001) 607.
3. J. Zhu et.al., Materials Science and Engineering A, 339 (2003) 53.
4. S. Tamirisakandala et.al., Scripta Materialia, 53 (2005) 1421.
5. S. Tamirisakandala et.al., Scripta Materialia, 53 (2005), 217.
6. R.O. Ritchie et.al., Metallurgical Transactions A, 10A (1979) 1557.
7. P.E. Irving et.al., Materials Science and Engineering, 14 (1974) 229.
8. K. Sadananda, A.K. Vasudevan, International Journal of Fatigue, 27 (2005) 1255.

**Table 1: Summary of the experimental results on Ti64-xB alloys**

<b>Alloy</b>	<b>(<math>\lambda</math>) (<math>\mu\text{m}</math>)</b>	<b>d (<math>\mu\text{m}</math>)</b>	<b><math>\sigma_y</math> (MPa)</b>	<b><math>\sigma_U</math> (MPa)</b>	<b><math>\epsilon_f</math> (%)</b>	<b><math>K_{Ic}</math> (MP a<math>\sqrt{\text{m}}</math>)</b>	<b><i>n</i></b>	<b><math>H_V</math></b>	<b>E (GPa)</b>	<b><math>\Delta K_0</math> (MPa <math>\sqrt{\text{m}}</math>)</b>	<b>m</b>
<b>Ti64</b>	14.1* $\pm 0.9$	1700*	833.9*	900.2*	6*	152*		325*	112*		
<b>Ti64- 0.05B</b>	8.04 $\pm 0.5$	233.4 $\pm 12.2$	925.9	972.2	8.9	72.9 $\pm 4.4$	0.056	373.6 $\pm$ 37.7	99.1 $\pm$ 3.5		
<b>Ti64- 0.10B</b>	5.5 $\pm 0.5$	152.5 $\pm 12.7$	928.7	974.8	7.2	62.6 $\pm 6.4$	0.036	386.1 $\pm$ 25	136.7 $\pm$ 12.7	8.43	3.76
<b>Ti64- 0.40B</b>	4.2 $\pm 0.2$	139.5 $\pm 11.2$	966.4	1012.2	6.0	38.0 $\pm 2.6$	0.028	410.5 $\pm$ 47.8	117.8 $\pm$ 6.9	6.64	3.78

\* Values taken from literature.

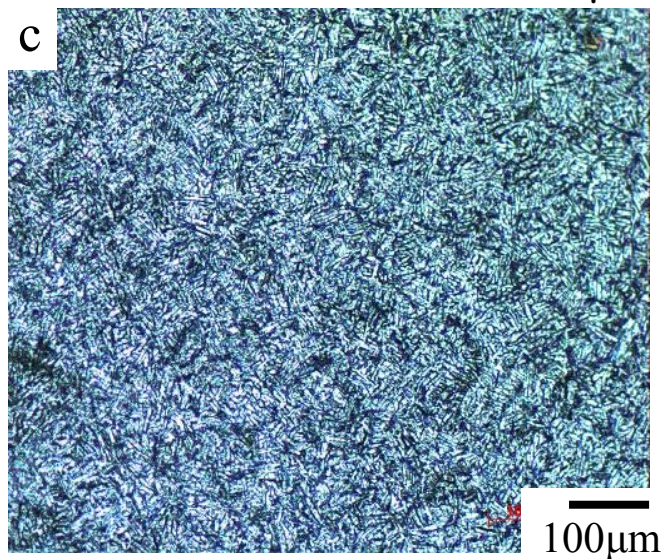
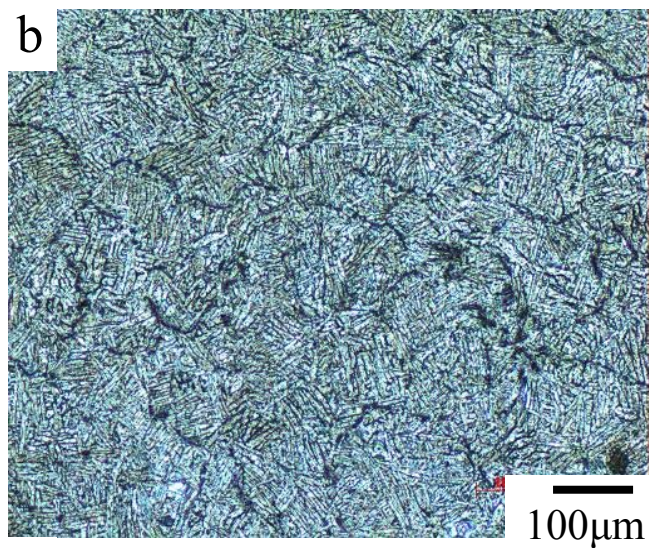
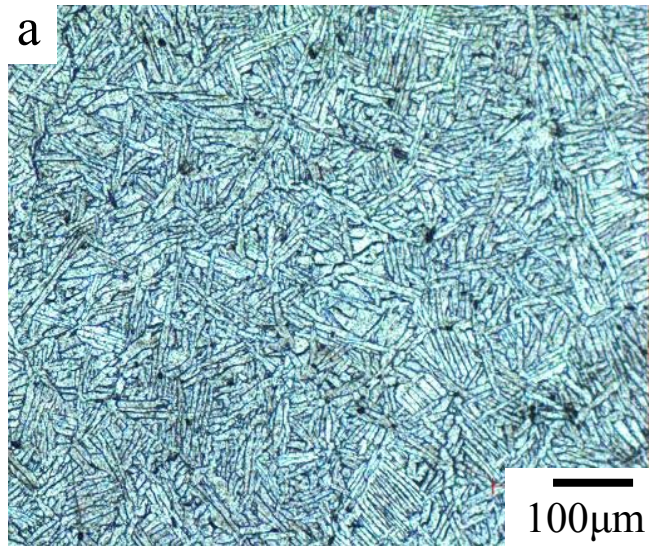


Fig 1: Optical micrographs of (a) 0.05, (b) 0.1 and (c) 0.4 wt % B added Ti64 at 100x showing TiB at grain boundaries

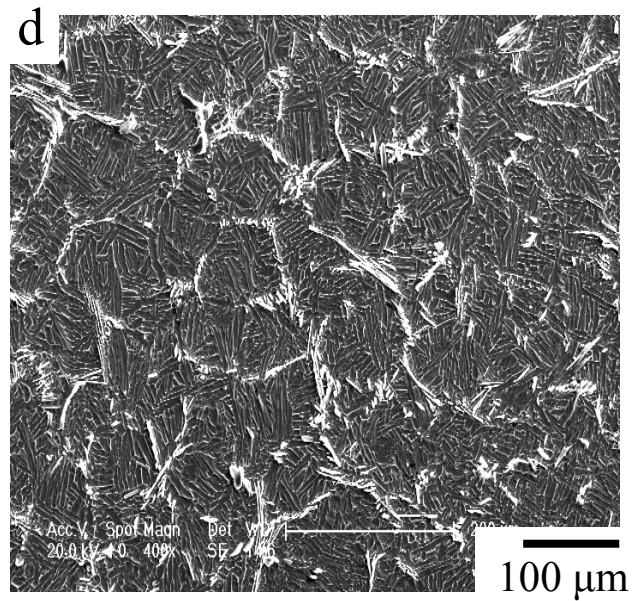
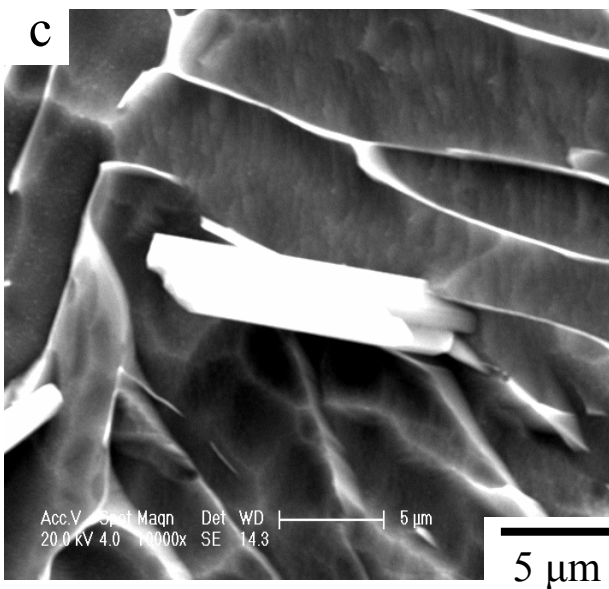
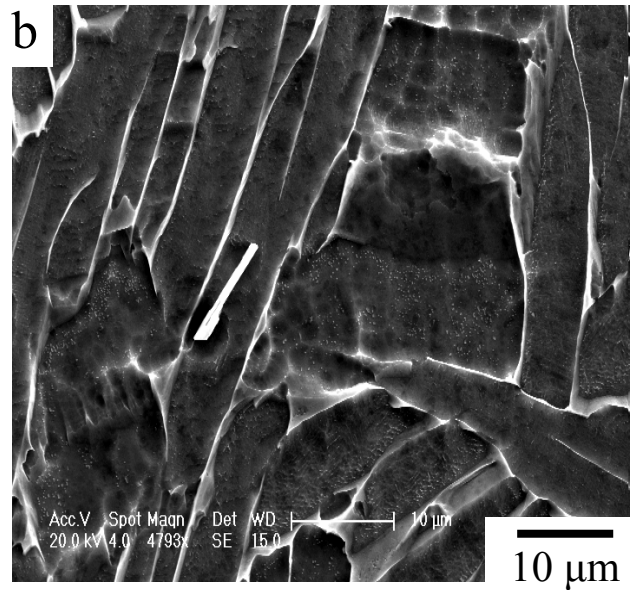
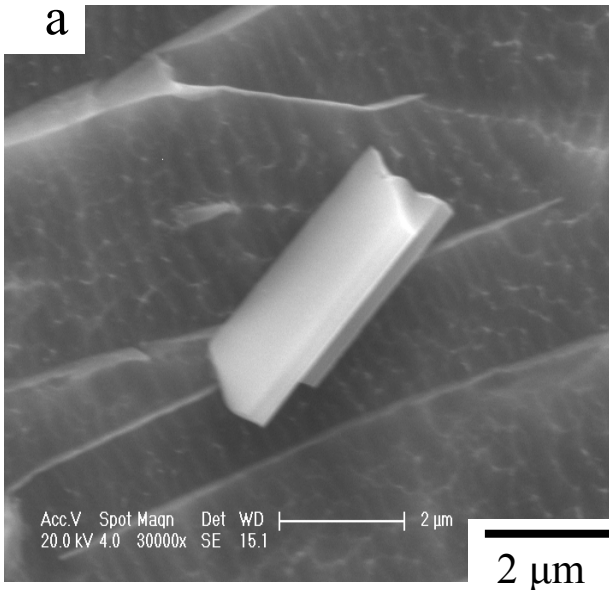


Fig 2: SEM of (a) 0.05, (b) 0.1 (c) 0.4 wt % B added Ti64 showing TiB needle morphologies and (d) Ti 64-0.4 B showing grain boundaries

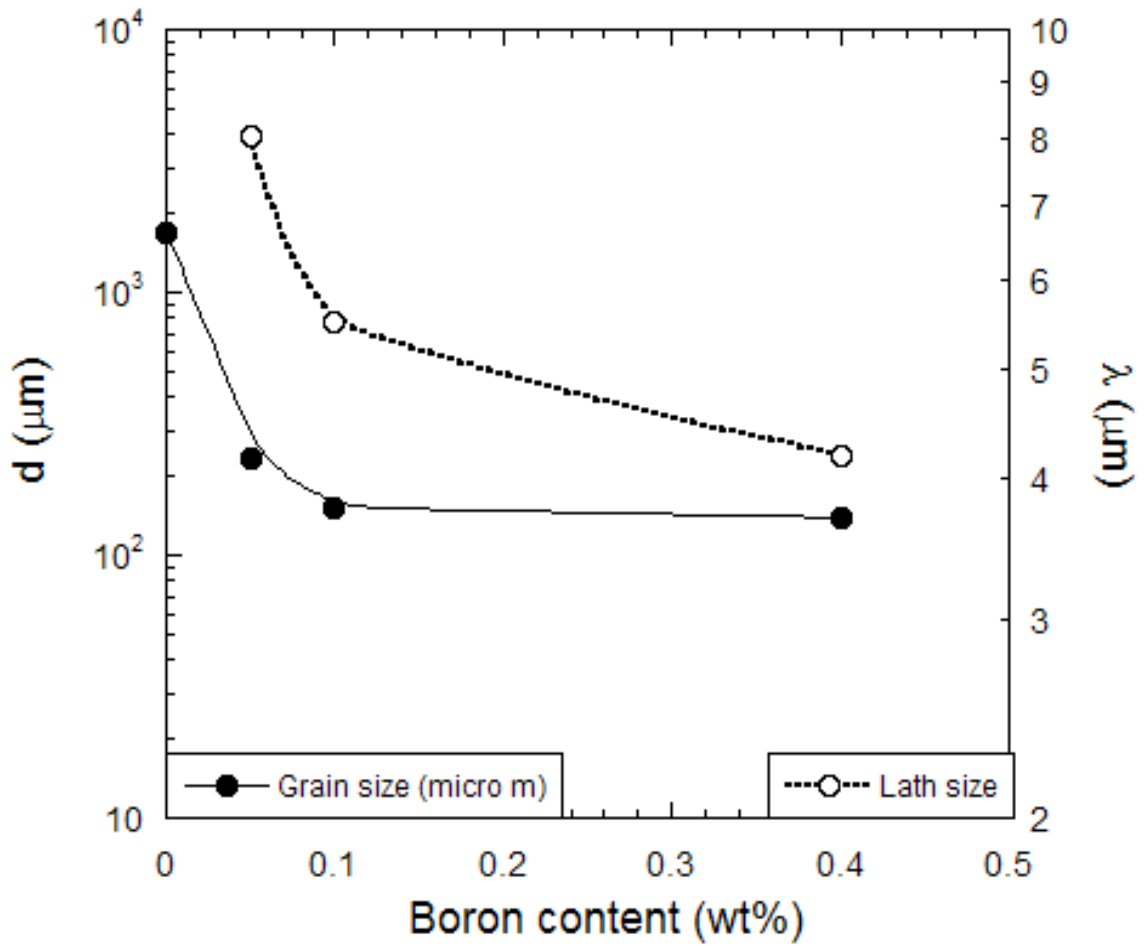


Fig 3: Grain size ( $d$ ) and lath size ( $\lambda$ ) variation of Ti64 with wt % B addition

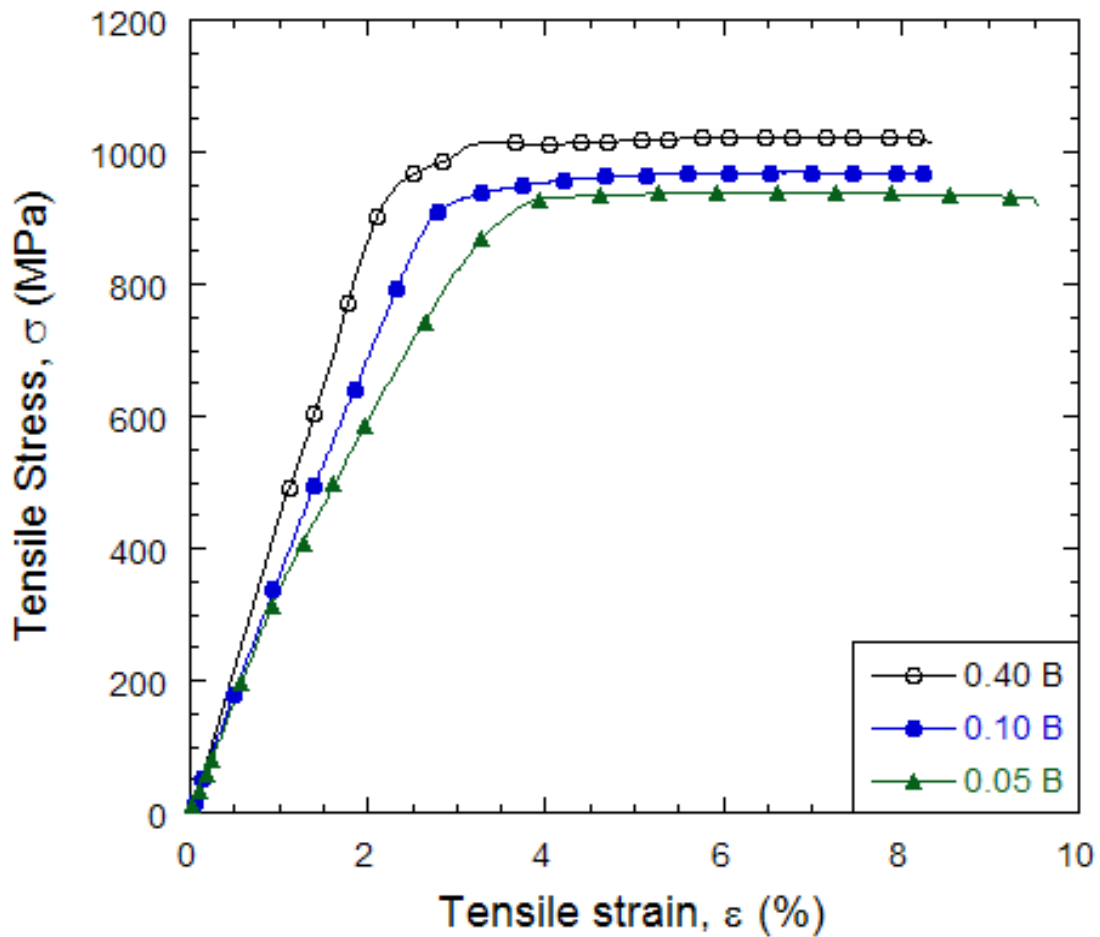


Fig 4: Tensile stress-strain variation of Ti64 with wt % B addition

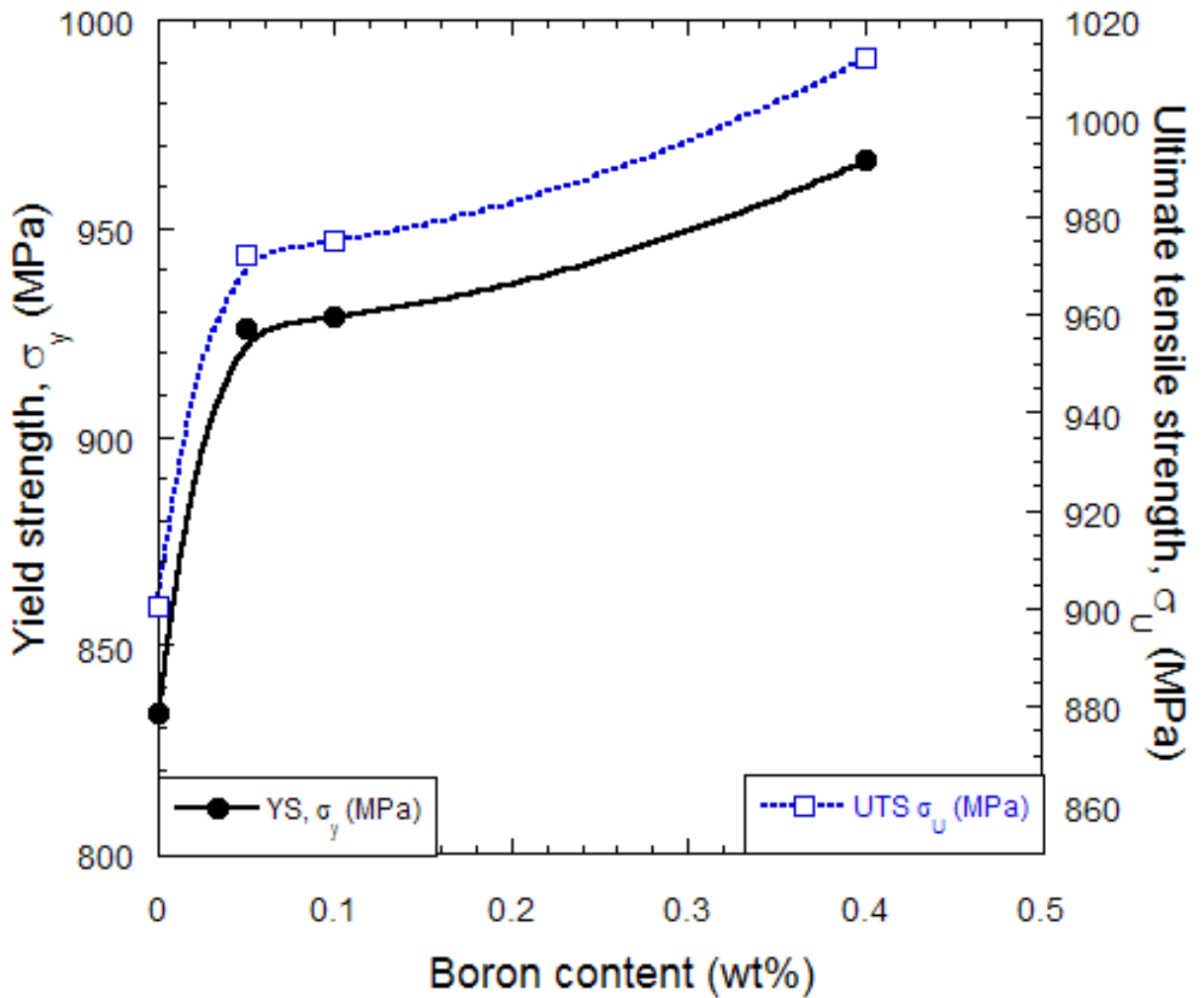


Fig 5: Variation of Yield strength and Ultimate tensile strength in Ti64 with wt % B addition

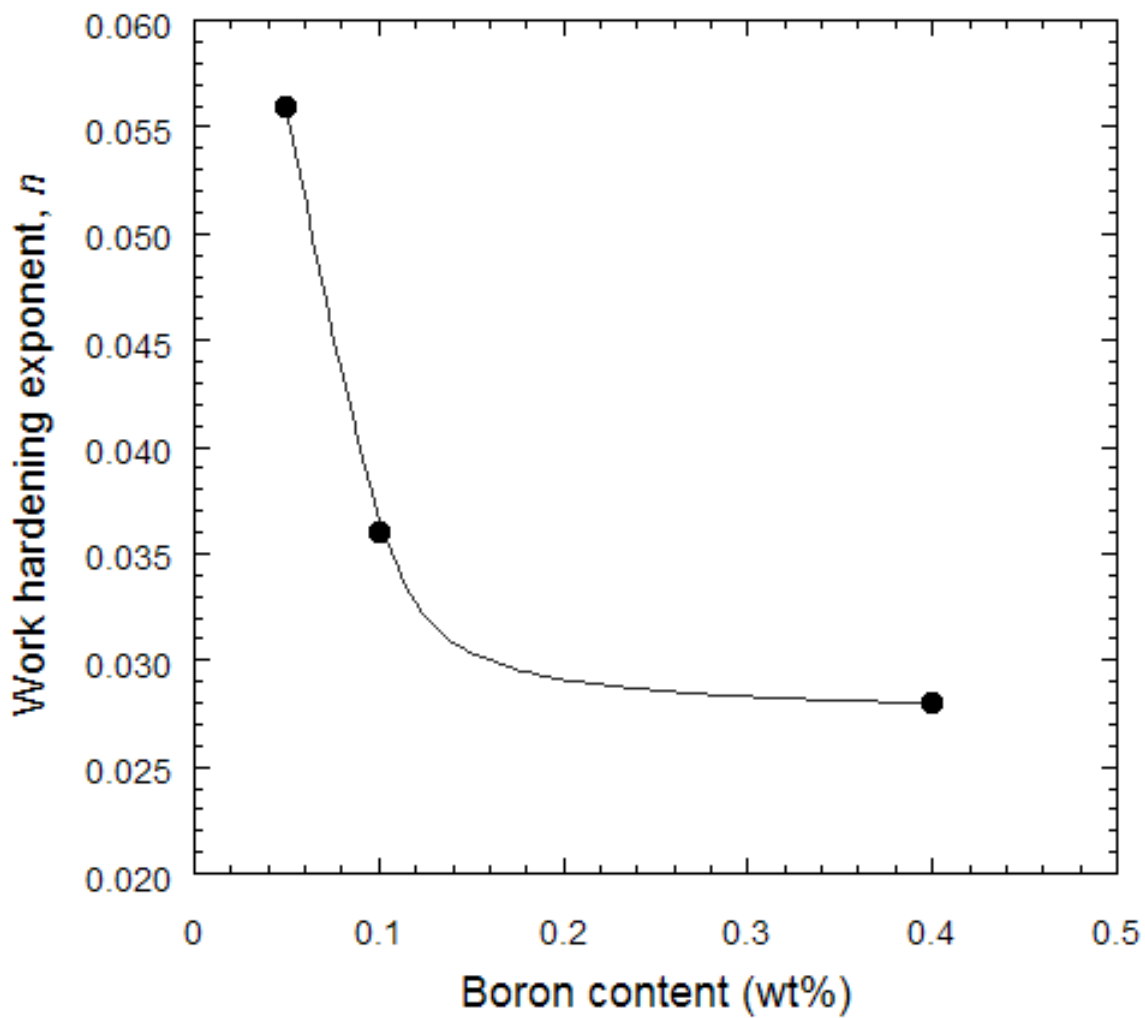


Fig 6: Variation of work hardening exponent,  $n$ , in Ti64 with wt % B addition

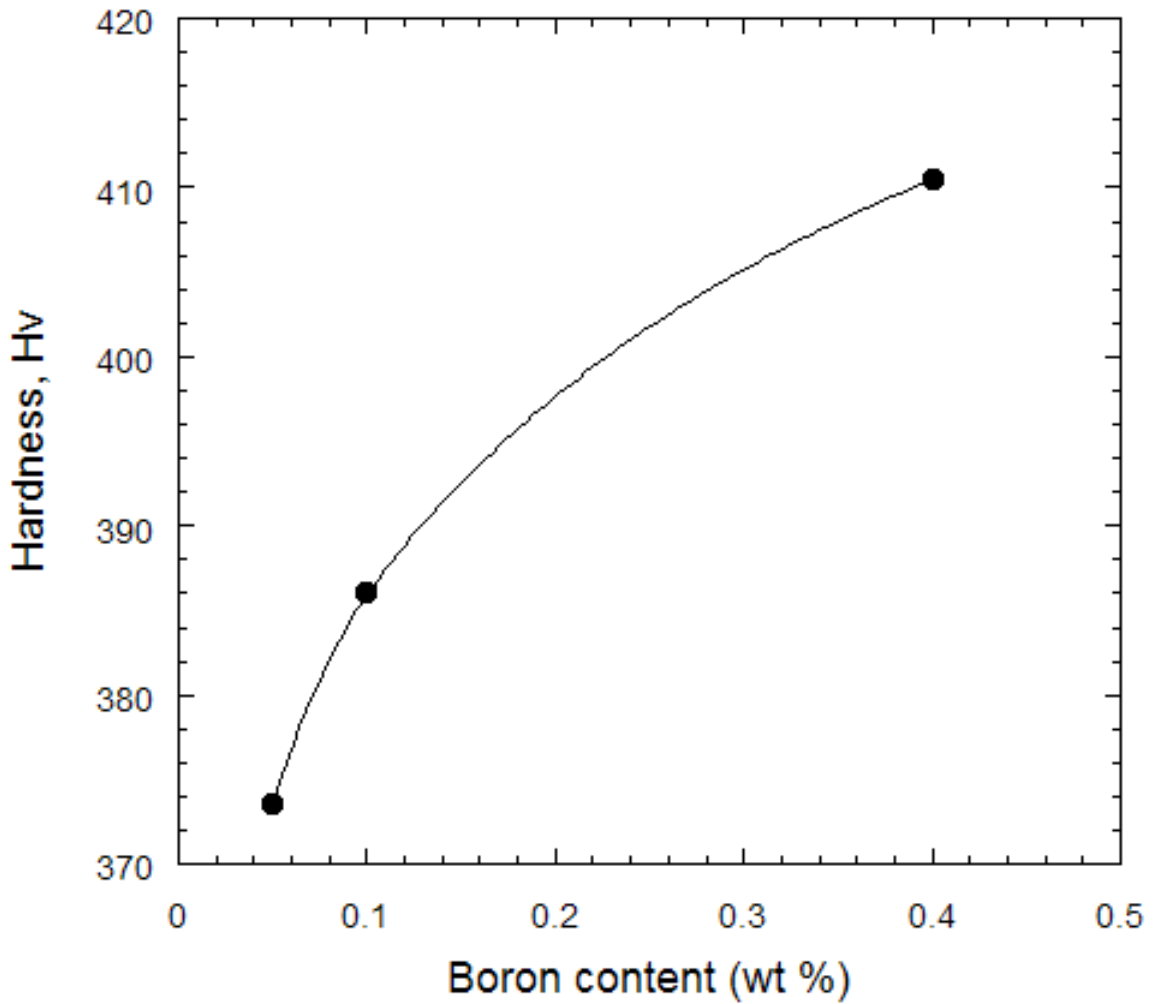


Fig 7: Variation of Instrumented Vickers microhardness,  $H_V$  in Ti64 with wt % B addition

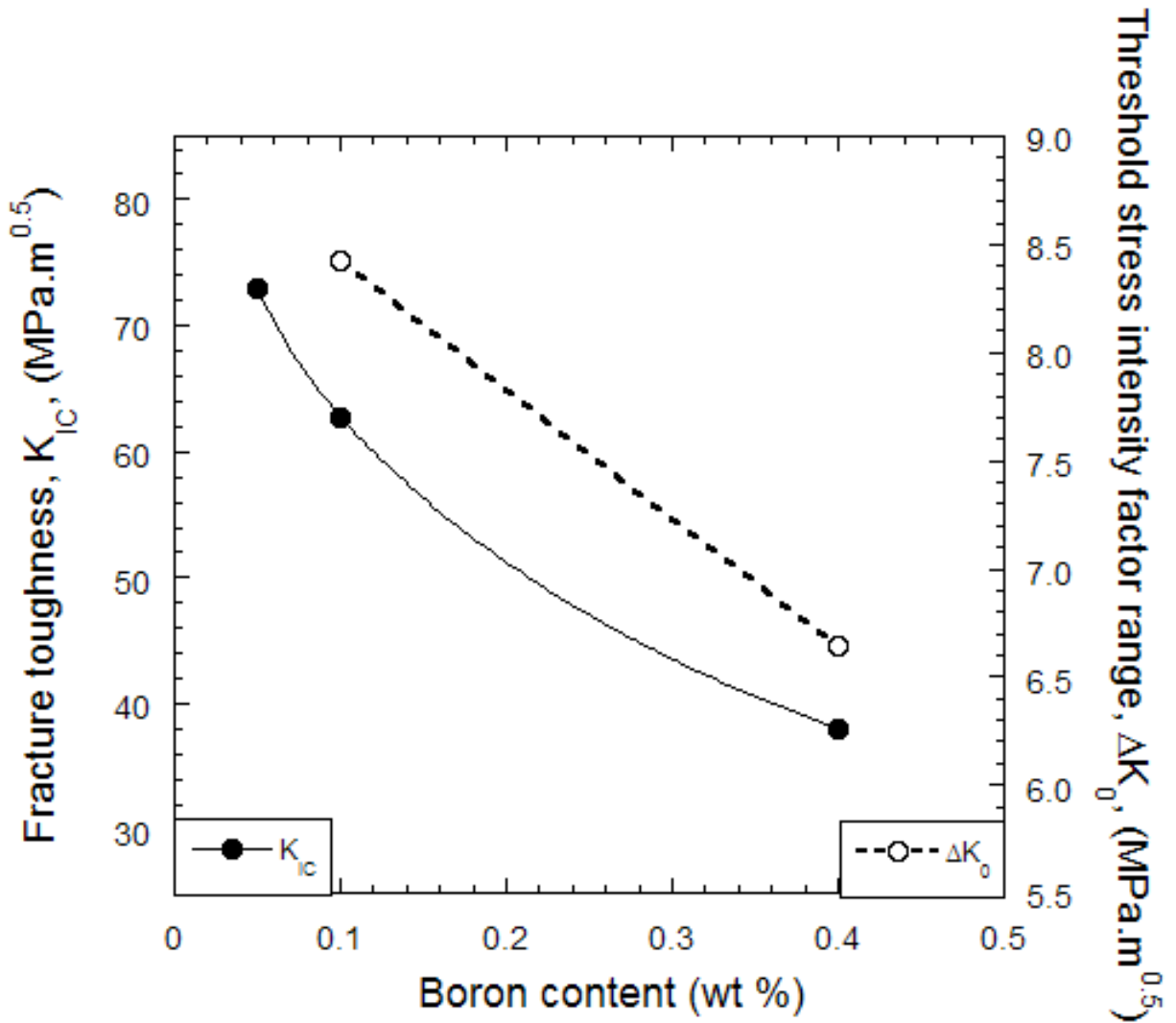


Fig 8: Variation of Fracture toughness and threshold stress intensity factor range values in Ti64 with wt % B addition

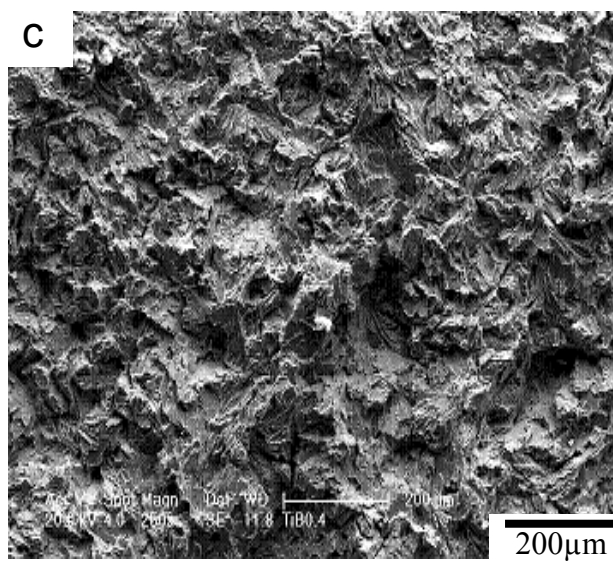
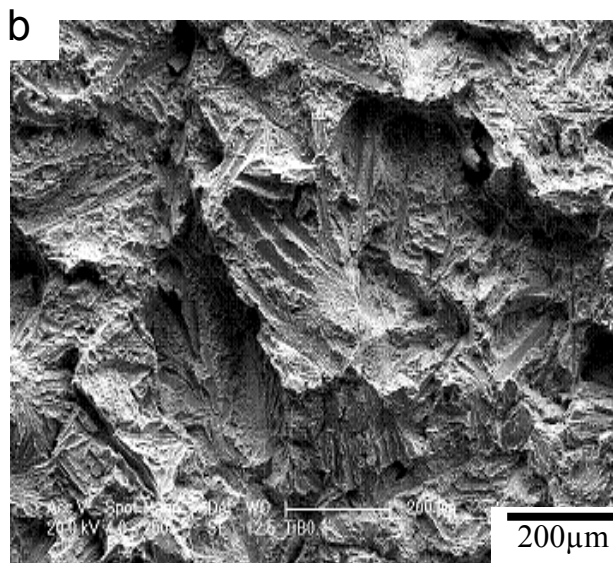
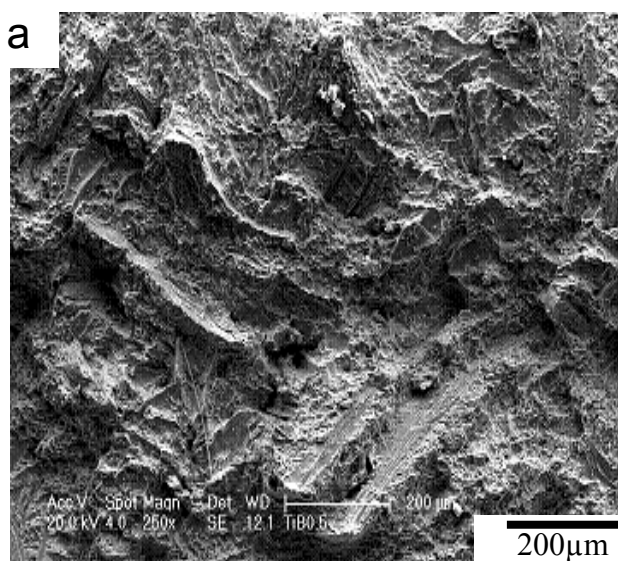


Fig 9: Fractographs of fracture toughness specimens of (a) 0.05, (b) 0.1 and (c) 0.4 wt % B added Ti64, at 250 x

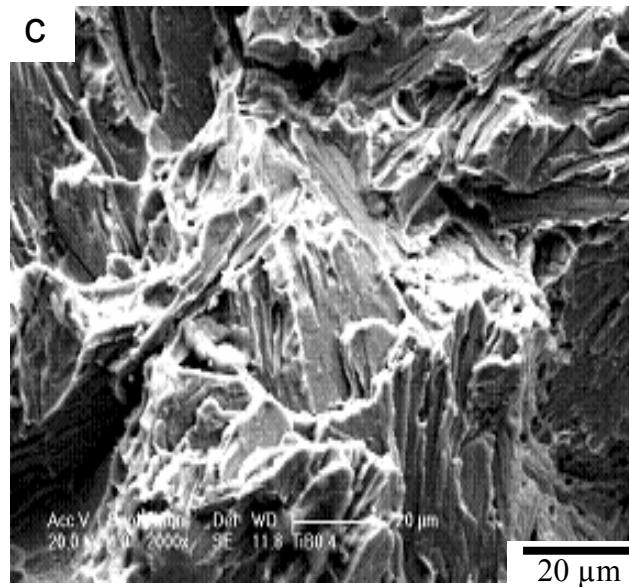
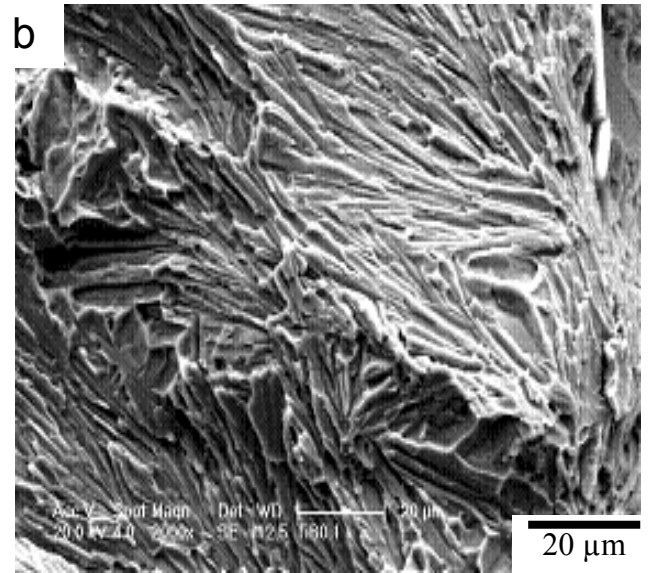
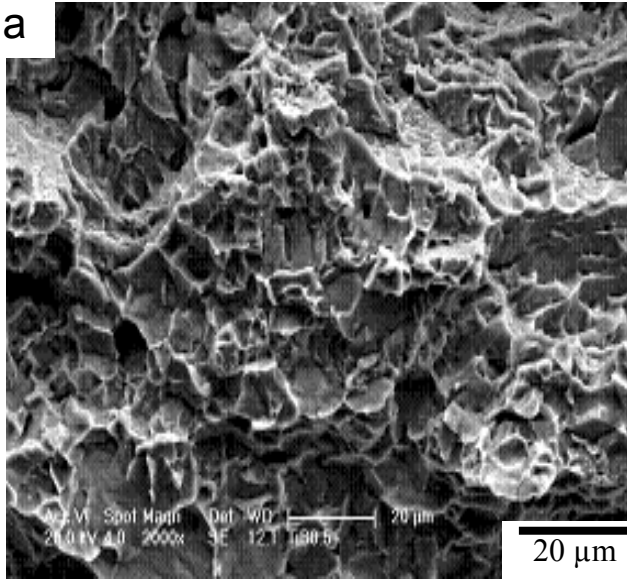


Fig 10: Fractographs of fracture toughness specimens of (a) 0.05, (b) 0.1 and (c) 0.4 wt % B added Ti64, at 2000 x

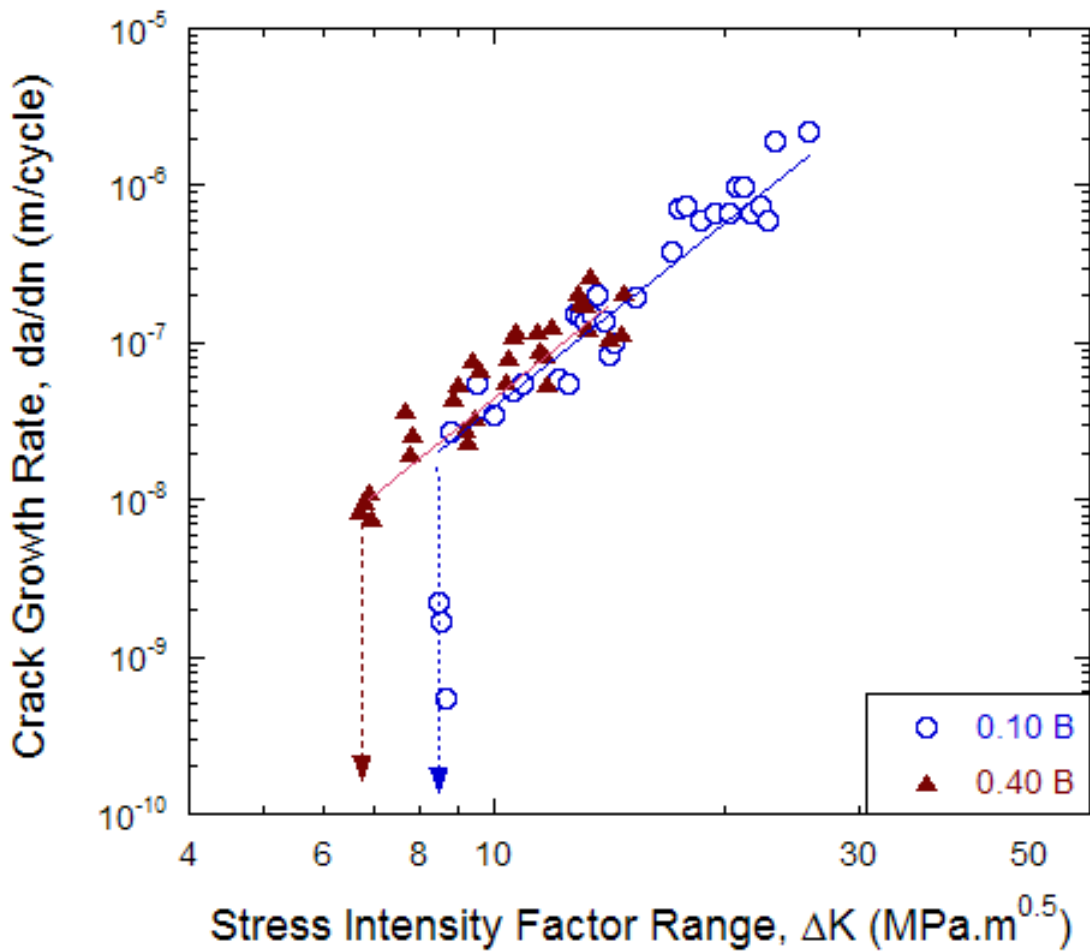


Fig 11: variation of fatigue crack growth rate with stress intensity factor range for 0.1 and 0.4 wt % B added Ti64

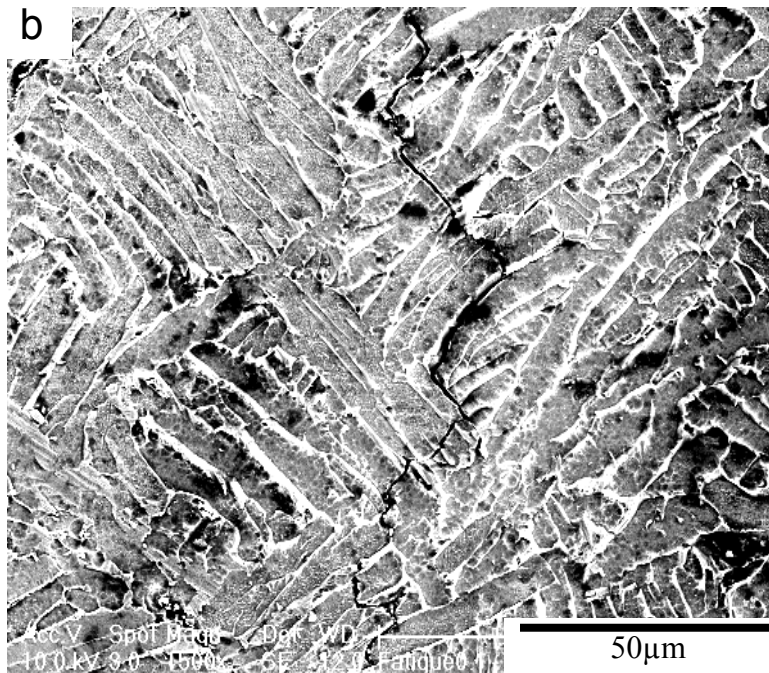
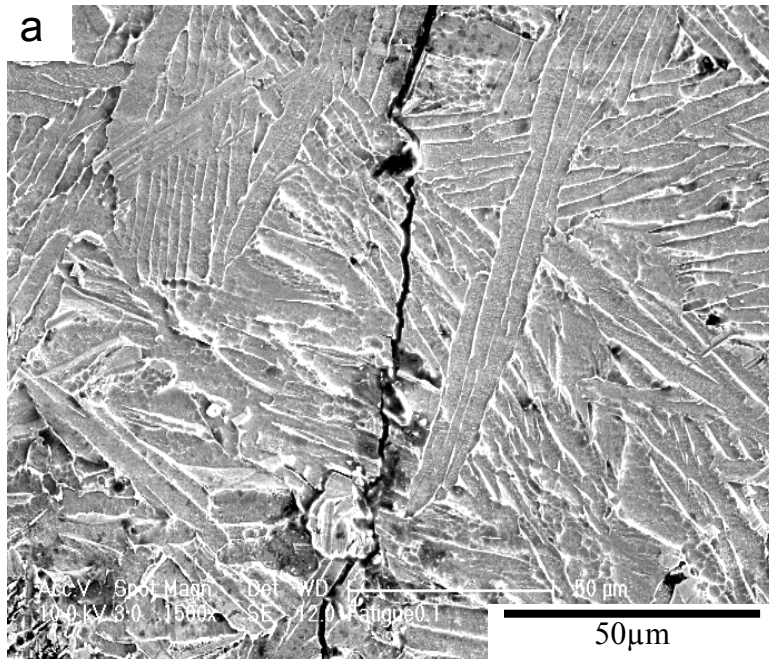


Fig 12: Fatigue crack propagation in Ti64-0.1 B at (a) Paris regime and (b) at near threshold region.